2021-05-04

Microplastics in the Lut and Kavir Deserts, Iran

Abbasi, S

10.1021/acs.est.1c00615
Environmental Science & Technology
American Chemical Society (ACS)

Microplastics in the Lut and Kavir Deserts, Iran

Sajjad Abbasi [a, *], Andrew Turner [b], Mohammad Hoseini [c], Hoda Amiri [d, e, *]

[a] Department of Earth Sciences, College of Science, Shiraz University, Shiraz 71454, Iran

[b] School of Geography, Earth and Environmental Sciences, University of Plymouth, PL4 8AA, UK

[c] Department of Environmental Health, Research Center for Health Sciences, Institute of Health, School of Health, Shiraz University of Medical Sciences, Shiraz, Iran

[d] Environmental Health Engineering Research Center, Kerman University of Medical Sciences, Kerman, Iran

[e] Department of Environmental Health, School of Public Health, Kerman University of Medical Sciences, Kerman, Iran

* Corresponding authors: sajjad.abbasi@shirazu.ac.ir;

hoda.amiri@gmail.com

https://doi.org/10.1021/acs.est.1c00615

Accepted April 1st 2021

Graphical Abstract

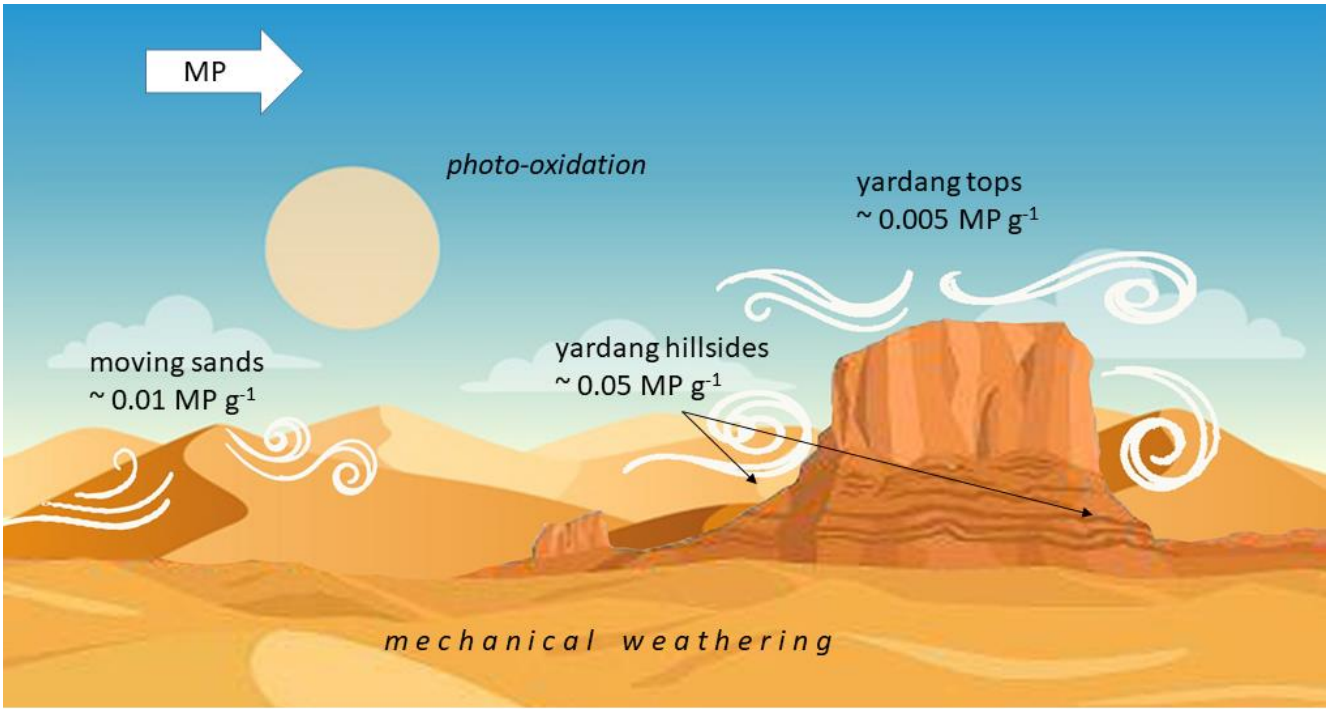

Abstract

Although microplastics (MP) are ubiquitous environmental contaminants, little is known about their occurrence and behaviour in remote, terrestrial environments. In this study, MP have been isolated from soils collected from various geomorphological features (yardangs, sand dunes, moving sands, seasonal lakes) of the Kavir and Lut Deserts on the Iranian plateau. The number of MP identified in 300 g samples ranged from zero (not detected) in several yardang tops to 25 on some yardang hillsides, with an overall average abundance of about 0.02 MP g^{-1}. The majority of MP were of a fibrous nature with a size distribution ($\leq$ 100 μm to $\geq$ 1000 μm) skewed towards the lower end, and analysis of a selection of particles by μ-Raman spectroscopy showed that polyethylene terephthalate and Nylon (polyamide) were the principal polymers. Scanning electron microscopy revealed intense degradation of some particles but limited weathering of others. With little evidence of meso- and macroplastics in the deserts, it appears that the majority of MP are brought into these environments from distant sources via the wind, with smaller, seasonal contributions from runoff associated with the adjacent mountains. It is proposed that some windborne MP are transported through the deserts relatively rapidly while others are subject to internal recycling and significant photo-oxidation and mechanical weathering.

Introduction

Microplastics (MP) have become increasingly studied in soils over the past few years because of their threats to terrestrial ecosystems [1, 2, 3]. Sources of MP in soils include littering and tipping, use of plastic-based mulches, application of sewage sludge, inundation by floodwater, road runoff and irrigation water, and atmospheric deposition [4, 5]. Soils are most contaminated by MP in the vicinity of population centers and certain industries or where intensive farming takes place [6, 7]. However, MP have also been detected in soils from regions remote from development, including Chilean rangelands and grasslands [8] and the Tibetan plateau [9]. Here, the principal means of contamination is believed to be the long-range aeolian transport of particles with air masses having origins in or passing through more developed regions [10]. Deposition may occur with dusts under dry conditions or with precipitation, with the relative significance of each pathways dependent on climate [11, 12]. Regardless of the mode of deposition, the capture and subsequent fate of MP are likely to be affected by the moisture content of the soil, either directly as a porous solid or indirectly by the nature and extent of vegetative cover [13].

One remote type of environment that has received very little systematic study in respect of MP is the desert, and in particular the subtropical desert. In the latter, conditions are likely to be amongst the most favorable for plastic degradation on the planet, with high (but variable) temperatures, high levels of insolation, and intense frictional forces and abrasion engendered by interactions between wind and sand. Zylstra [14] reported on the distributions of plastic bags and balloons in the Sonoran Desert, Arizona, and proposed that such items might be a source of MP through photodegradation. However, and more generally, external, airborne sources of MP in deserts have thus far not been considered.

In the present study, soils were collected from two remote, subtropical deserts in Iran in order to determine the presence, quantities and characteristics MP in this type of environment. Specifically, samples were collected from different geomorphological features and on a monthly basis throughout the year and MP isolated, categorized and analysed using established techniques. The broad origins of the MP were also investigated by computing back trajectories from the study regions.

Experimental section

Sampling sites

Two deserts on the Iranian plateau (Figure 1) were considered in the present study whose climates and geomorphologies are described in detail elsewhere [15, 16, 17] and are summarized as follows. The Dasht-e-Kavir (Kavir) occupies about 80,000 km^2 and has a minimum elevation of 800 m. It is characterized by pebbly steppes and salt deserts and, in the northern reaches, sand dunes and shifting sands. Northerly winds transport sand to the southwest of the region, but much of the desert is covered with grey-colored calcareous soils. The Dasht-e-Lut (Lut) occupies about 50,000 km^2 and lies between about 100 m and 500 m in elevation. It is hyperarid and is largely made up of gravel and sandy desert. Strong northerly and northwesterly winds blow sand southwards, and in particular between June and October, forming dunes and shifting sands. Both deserts are characterized by long and hot summers (with temperatures often exceeding 50^oC), but winter runoff from surrounding mountains can create seasonal lakes or marshes. Because of the harsh conditions, communities are generally limited to the peripheries of the deserts.

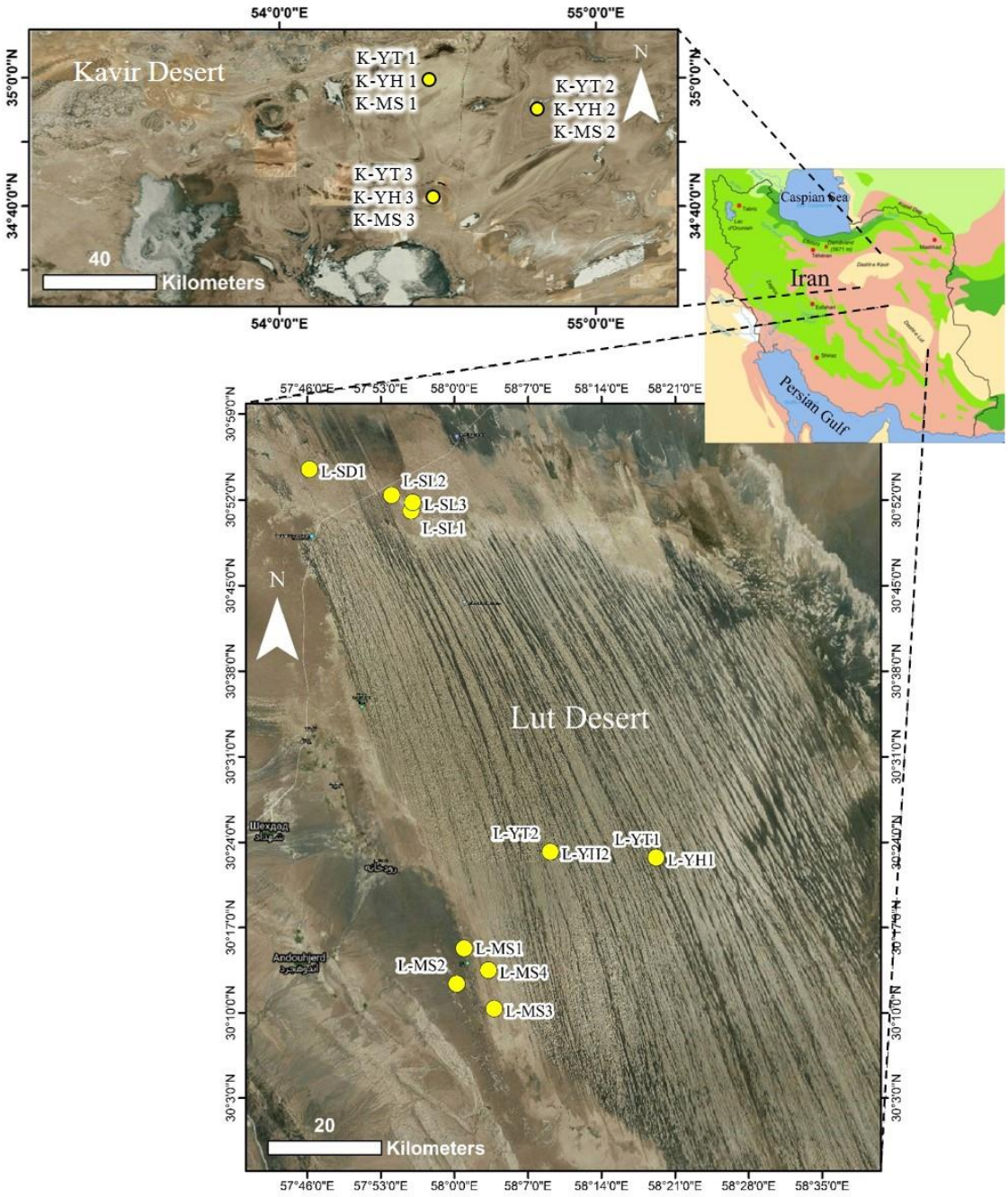

104

105 Figure 1: Locations of the soil samples taken in the Kavir (K-) and Lut (L-) deserts. YT = yardang

106 top; YH = yardang hillside; MS = moving sand; SD = sand dune; SL = seasonal lake. UTM

107 coordinates of the sampling locations are shown in Table S2.

108

109

110 *Sampling*

111 With the assistance of the Kerman Tourist Guides Association, deserts were accessed in an off-
112 road vehicle through the main and subsidiary road network, with sampling locations usually 300-
113 500 m away from the access road. Samples were taken from the locations shown in Figure 1 by an
114 operator wearing cotton clothing and at a suitable distance (> 50 m) from and upwind of the off-
115 road vehicle.

116 An initial sampling campaign consisted of the collection of 21 sandy to clayey soils from the Kavir
117 and Lut deserts during the dry season (September 2019). Geomorphological features considered
118 were moving sands, yardang tops (up to 50 m in elevation) and yardang hillsides (Kavir and Lut),
119 and sand dunes and seasonal lakes (Lut only). About 300 mL of topsoil (depth < 5 cm) was
120 collected with a metallic trowel and transferred into a pre-cleaned glass jar, with the trowel cleaned
121 with filtered water between samples. Sample jars were covered with Al foil and transported to the
122 laboratory where microplastic extraction and identification was undertaken according to protocols
123 described below. Additionally, and between October 2019 and August 2020 in the Kavir desert,
124 sampling continued towards the end of each month at the locations and geomorphological features
125 shown in Figure 1.

126

127 *Sample treatment and microplastic extraction*

128 In a clean laboratory, soil samples were transferred to individual, 600-mL glass beakers using a
129 stainless steel spoon and dried for 24 h at 25ºC. Dried samples were sieved through a 5-mm
130 stainless steel mesh to remove coarse material like stones and plant debris (and identify any meso-

plastics) before being stored in clean 600-mL glass beakers that were covered with Al foil. Organic matter was destroyed by oxidation of 300 g of each sample with 200-300 mL of 30 % H_2O_2 (Arman Sina, Tehran) at room temperature until bubble formation ceased. Residual material was washed through a 150 mm diameter S&S filter paper (blue band, grade 589/3, 2 µm pore size) using filtered, deionized water before being dried in a sand bath at 60°C for 2 h. MPs were subsequently separated by flotation for 24 h in a saturated 300 mL solution of $ZnCl_2$ (Arman Sina, Tehran; density 1.6 – 1.8 g cm^{-3}) in clean glass beakers after an initial 5-min period of agitation at 350 rpm. Decanted contents were subsequently centrifuged for 5 min at 4000 rpm and supernatants vacuum-filtered through S&S filter papers. To ensure maximum recovery of MP, this process was repeated twice, with resulting filters air-dried for 48 h at 25°C in a clean room under laminar flow and transferred to glass Petri dishes for physical and chemical characterisation.

Microplastic identification

MP on filters were visually identified and counted under a binocular microscope (Carl-Zeiss) at up to 200 x magnification using a 250 µm stainless steel probe and ImageJ software, with identification criteria based on thickness and cross sectional properties, shininess, hardness, reaction to a hot needle, and surface structure [18]. Size was recorded according to length along the longest axis, L ($L \leq 100$ µm, $100 < L \leq 250$ µm, $250 \leq L < 500$ µm, $500 \leq L < 1000$ µm, $L \geq 1000$ µm), color was categorized as black-grey, yellow-orange, white-transparent, red-pink or blue-green, and shape or type was classified as fibre, primary (pellet, granule) or secondary (fragment, film).

Surface and morphological characteristics, chemical composition and polymeric construction were determined on a range of randomly selected MP from different locations and of different color,

size and form (n = 21) using a μ-Raman spectrometer and scanning electron microscope (SEM). The μ-Raman spectrometer (LabRAM HR, Horiba, Japan) employed a laser of 785 nm and Raman shift of 400-1800 cm^{-1} with acquisition times between 20 and 30 s. The polymeric composition of the sample was determined by comparing the vibrational spectrum with reference spectra in the instrument library and using a threshold match criterion of 0.80. The high vacuum SEM (TESCAN Vega 3, Czech Republic) was operated with a resolution of 2 nm at 20 kV and equipped with an energy-dispersive X-ray microanalyser (EDX). Here, MP were mounted on double-sided copper adhesive tape on microscope slides and gold-coated.

Quality control

Laboratory equipment and containers were washed with phosphate-free soap, double rinsed with filtered water and soaked in 10% Merck Suprapur HNO_3 for 24 h before being rinsed twice with double-distilled water, dried at room temperature in a clean room and, where appropriate, protected by Al foil. Laboratory benches were cleaned thoroughly with ethanol, laboratory clothing was cotton-based and all reagents and solutions were filtered through S&S blue band filters before being used. Controls, consisting of open-air blanks processed as above, revealed no airborne MP contamination.

MP recovery was also checked by adding ten MP of distinctive color, size and shape, and prepared by milling of polyethylene terephthalate (PET), polyethylene, polypropylene and polyvinyl chloride, to a 300 g sample of desert soil. The amended sample was processed as above and the ten customized MP were successfully isolated and identified under the microscope.

Trajectory calculations

In order to assess the potential source range of MP to the study locations in the Kavir and Lut deserts, 48-h back trajectories were calculated using the National Oceanic and Atmospheric Administration online software, Hybrid Single Particle Lagrangian Integrated Trajectory (HYSPLIT) and Global Forecast System (0.25 degree global) meteorological data. Trajectories were calculated at six-hour intervals at a height of 500 m above ground level and a resolution of 1 degree and were integrated as frequency distributions for each month preceding the sampling date.

Results

Examples of MP retrieved from the desert soils and as viewed under the binocular microscope are shown in Figure 2. The majority of particles were fibres of varying length, thickness and color that were often coiled or twisted. Of the 21 MP retrieved from Kavir and Lut soils and analysed for polymeric makeup by μ-Raman spectroscopy (and comprising 18 fibres and three fragments), eleven were identified as PET, seven were Nylon, two were polystyrene and one was polypropylene.

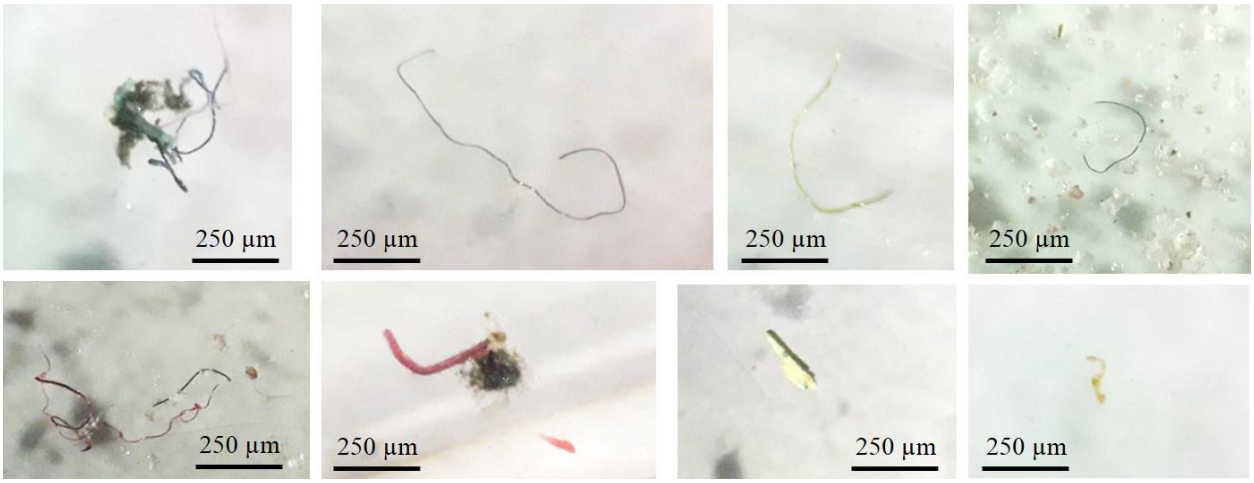

Figure 2: Microscopic images of selected fibrous and fragmented MP sampled from the Kavir and Lut deserts.

Under the SEM, and as exemplified in Figure 3, the surfaces of some of the fibres examined appeared smooth but with adhered particulates returning EDX peaks (e.g., Al, Ca, Cl, Fe, Mg, Ti, Zn) characteristic of soil and, possibly, residual salts (including $ZnCl_2$) that formed during sample processing. Other fibres, however, along with fragmented MP, appeared to have undergone significant and heterogeneous weathering and fragmentation, resulting in surfaces that were rough and irregular and, in some cases, pitted and notched, but that still contained evidence of adherent or trapped soil particulates.

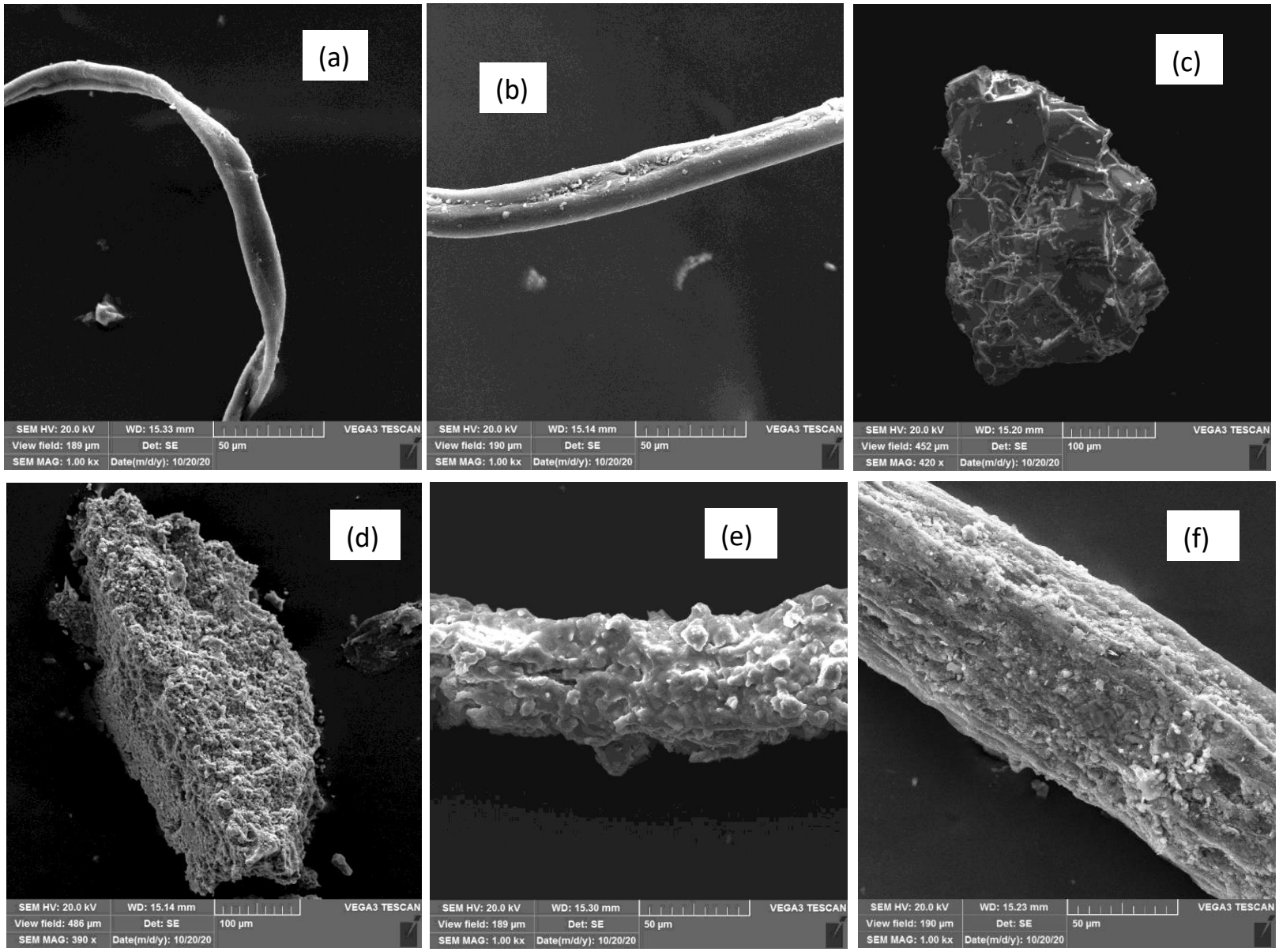
(a)
SEM HV: 20.0 kV
WD: 15.33 mm
VEGA3 TESCAN
View field: 189 µm
Det: SE
50 µm
SEM MAG: 1.00 kx
Date(m/d/y): 10/20/20
(b)
SEM HV: 20.0 kV
WD: 15.14 mm
VEGA3 TESCAN
View field: 190 µm
Det: SE
50 µm
SEM MAG: 1.00 kx
Date(m/d/y): 10/20/20
(c)
SEM HV: 20.0 kV
WD: 15.20 mm
VEGA3 TESCAN
View field: 452 µm
Det: SE
100 µm
SEM MAG: 420 x
Date(m/d/y): 10/20/20
(d)
SEM HV: 20.0 kV
WD: 15.14 mm
VEGA3 TESCAN
View field: 486 µm
Det: SE
100 µm
SEM MAG: 390 x
Date(m/d/y): 10/20/20
(e)
SEM HV: 20.0 kV
WD: 15.30 mm
VEGA3 TESCAN
View field: 189 µm
Det: SE
50 µm
SEM MAG: 1.00 kx
Date(m/d/y): 10/20/20
(f)
SEM HV: 20.0 kV
WD: 15.23 mm
VEGA3 TESCAN
View field: 190 µm
Det: SE
50 µm
SEM MAG: 1.00 kx
Date(m/d/y): 10/20/20

Figure 3: SEM images of six MP retrieved from the Kavir and Lut deserts. (a) A smooth, yellow Nylon fibre from a yardang top contaminated with soil particulates; (b) a smooth, white polyethylene terephthalate fibre from a yardang top contaminated with soil particulates; (c) an abraded, pink fragment of unknown polymeric composition from a yardang hillside and contaminated by soil particulates; (d) a weathered, white polypropylene fragment from a yardang hillside; (e) a weathered, green polystyrene fibre from a yardang hillside; and (f) a weathered, yellow polyethylene terephthalate fibre from a yardang hillside.

A summary of the numbers and types of MP identified in the 300-g soil samples collected from the different locations and geomorphological features in the Lut Desert in September 2019 is given in Table 1. There were 67 MP in total, with fibres dominating shape or form (96%) and the three non-fibrous MP classified as fragments. Features with the greatest number of MP were the hillsides of the yardangs and two out of the four moving sands. Moreover, yardang hillsides and moving sands were the only features where MP fragments were observed. Nineteen MP, that included two fragments, were in the smallest size category ($L \leq 100$ μm) and four MP were in the largest category ($L \geq 1000$ μm); six samples were white or transparent, 27 were black or grey and the remainder consisted of a variety of colors (but mainly red/pink and blue/green and that included all fragmented MP).

Table 1: Number of MP and their type, size and color distribution in 300-g soil samples from each site in the Lut desert, sampled in September 2019. YT = yardang top; YH = yardang hillside; MS = moving sand; SD = sand dune; SL = seasonal lake.

sample	MP	fibres	L ≤ 100 µm	L ≥ 1000 µm	white-transp	black-grey
L-YT1	4	4	2	1	1	2
L-YT2	2	2	1	0	0	2
L-YH1	9	8	3	0	0	4
L-YH2	13	12	1	0	3	3
L-SD1	3	3	2	0	1	0
L-MS1	16	16	3	1	0	9
L-MS2	3	2	1	0	0	1
L-MS3	1	1	1	0	0	1
L-MS4	6	6	3	1	0	4
L-SL1	3	3	2	0	0	1
L-SL2	4	4	0	0	0	0
L-SL3	3	3	0	1	1	0
total	67	64	19	4	6	27

Figure 4 shows the average number of MP identified in the soils from the three yardang tops, yarding hillsides and moving sands in the Kavir desert that were sampled monthly over a year-long period. MP were most abundant in hillside soils throughout, with a distinct maximum occurring in February-March. Table 2 presents the total number of MP identified in the Kavir desert each month, along with abundance according to type, color and size. There were no clear temporal trends in these data and, overall, 617 MP were detected with an average abundance on a number basis of 0.02 g^{-1}. Over 93% of MP were of a fibrous nature (with the remainder fragments or films), white-transparent was the most common color, and twice as many particles were present in the finest size fraction (L ≤ 100 µm) than in the coarsest fraction (L ≥ 1000 µm).

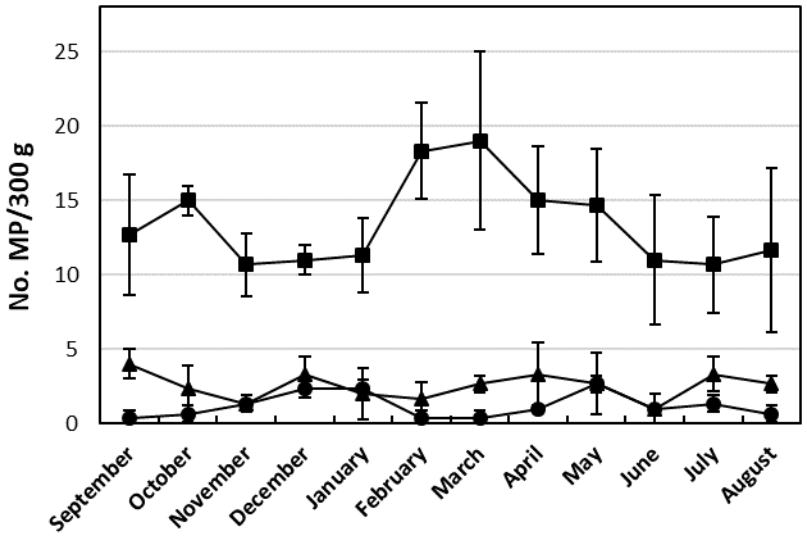

Figure 4: Average number of MP in 300-g soils sampled from yardang tops (●), yardang hillsides (■) and moving sands (▲) each month over a twelve-month period in the Kavir desert. Errors represent one standard deviation (n = 3).

Table 2: Total number of MP and their type, color and size distributions in the nine, 300-g Kavir desert soils (three each from yardang tops, yardang hillsides and moving sands) sampled over twelve months.

MP	September	October	November	December	January	February	March	April	May	June	July	August	total	%
total	51	54	40	50	47	61	66	58	60	39	46	45	617	100
fibres	45	48	37	49	45	57	62	53	59	39	40	42	576	93.4
fragments	6	3	2	1	2	3	3	3	1	0	3	2	29	4.7
films	0	3	1	0	0	1	1	2	0	0	3	1	12	1.9
white-transp	18	17	16	24	17	27	28	23	25	17	16	23	251	40.7
black-grey	13	14	9	12	9	14	25	19	20	13	12	8	168	27.2
other colours	20	23	15	14	21	20	13	16	15	9	18	14	198	32.1
L ≤ 100 µm	11	14	20	17	11	20	22	16	19	12	12	11	185	30.0
L ≥ 1000 µm	7	5	6	10	8	10	10	12	11	6	6	4	95	15.4
other sizes	33	35	14	23	28	31	34	30	30	21	28	30	337	54.6

Forty eight-hour back trajectory frequencies calculated using HYSPLIT for the Lut Desert in September 2019 are shown in Figure 5. Frequencies (> 1%) extend in all directions with a range of about 1500 km to the west and northwest. However, the highest frequencies (> 50%) are associated with air masses from the northwest to northeast and with a range of about 300 to 600 km. Monthly model frequency outputs for the Kavir Desert are shown in Figure S1 of the

supporting information. The ranges of frequencies above 1% and above 50% are broadly similar to those reported for the Lut Desert. However, there is a distinct seasonal pattern to trajectory direction, with air from the north and northeast dominating from May to November and a notably greater westerly component from December to April.

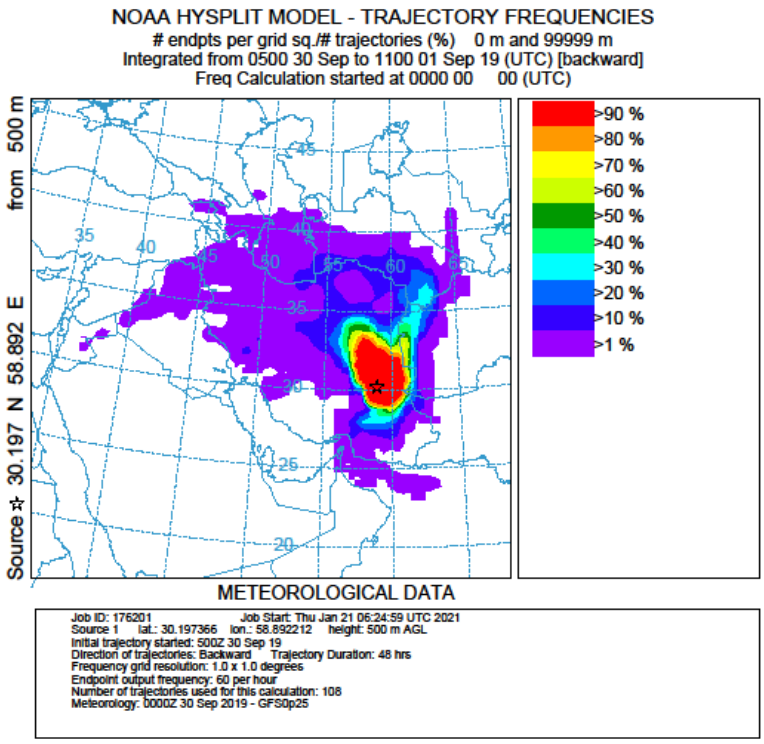

Figure 5: Frequencies of air trajectories crossing a given area and arriving at the sampling locations in the Lut desert for September 2019, calculated from 48-hour air mass back-trajectories using HYSPLIT.

Discussion

MP have been detected in various remote environments, including the deep ocean [19], protected wildernesses of the USA [10], mountain basins [20] and the Arctic [21], but this paper is the first to report

their occurrence in the subtropical desert. Here, MP are dominated by fibres of various colors and sizes (but skewed towards the lowest size fraction considered), with no granules, pellets or other primary MP detected and no evidence of any larger (meso-) plastics amongst the samples. The latter observation, and only occasional sightings of plastic litter (mainly bags) trapped behind vegetation during the sampling campaigns, suggests that the majority of MPs are not formed in situ through degradation and fragmentation but have been brought directly into the desert regions from external sources. Moreover, the dominance of fibrous MP, whose relatively high surface area to volume ratio increases drag forces and reduces settling velocity, suggests that wind is the principal vector of transportation [21,22]. Aeolian transportation-deposition is consistent with the greater occurrence of MP on the hillslopes of yardangs, where enhanced particle deposition takes place [23], and more generally, a size distribution that is skewed towards the fine end [20, 24, 25]. This is in contrast to many other remote regions where water is a more important vector for transportation and deposition and the stock of soil-borne MP is dominated by fragments and films [26, 9.]

Recent estimates suggest that airborne MP fibres are capable of being transported up to 1000 km from their point of origin [10] and that tire-wear particles, albeit shorter than the MP fibres reported herein but of greater density and lower drag, may have atmospheric residence times ranging from 5.5 to 11 days [27]. With MP subject to long-range transport and atmospheric residence times on the order of days and with limited scope for washout with precipitation, 48-hour back trajectory calculations would appear to provide a reasonable indicator of particle origin in the current study. Trajectories for the Kavir desert (Figure S1) suggest that MP are largely transported from more populated and developed (including agricultural) regions to the north and northeast from May to November, with a greater contribution from regions to the west from December to May.

Although wind appears to be the principal mode of transportation of MP into and within the deserts, an additional, seasonal source that is likely more locally significant is the surrounding mountains. Here, MP that have been deposited in the catchment locally or from farther afield are carried, via winter runoff, into the peripheral regions of the deserts and into the seasonal lakes and marshes. The ten MP retrieved from the seasonal lakes of the Lut did not, however, exhibit any clear differences to MP collected from other regions and geomorphological features of the desert.

The number of MP identified in 300 g of dry desert soil ranged from zero (not detected) in several yardang tops to 25 on some yardang hillsides. The latter is equivalent to 0.083 MP g^{-1}, and on this basis the overall average abundance of MP in soils from the Kavir and Lut deserts is about 0.02 MP g^{-1}. Comparing this value with literature concentrations reported for soils remote from population centers or not contaminated by agricultural or industrial practices or by floodwater is not straightforward. This is because discrepancies exist in sampling design (e.g. soil volume), sample processing (e.g. sieve size and use or means of removal of organic matter and plastic flotation), operational definitions of MP and methods of and criteria for MP identification, and the nature and degree of data reporting. Nevertheless, the average value derived herein for desert soil is at the low end of the range of MP concentrations reported for Tibetan plateau soils (0.02 to 0.11 MP g^{-1}; [9]) and soils from remote regions of the Fars province of southern Iran (~ 0.1 MP g^{-1}; [28]) and is an order of magnitude below the maximum concentrations reported for Swiss floodplain soils (0.59 MP g^{-1}; [26]) and Chilean grassland and rangeland soils (0.2 MP g^{-1}; [29]). Lower concentrations of MP in desert soils may be attributed to relatively little input via rainfall washout [11], dilution by a large stock of unconsolidated and mobile soil and sand particles, and the harsh environmental conditions that act to weather MP into sizes that evade deposition or detection by conventional means.

Specific conditions that particles, including MP, are exposed to in the desert include high levels of UV radiation, high temperatures (that can exceed 80 ºC in sand) and intense, wind-assisted mechanical abrasion and sandblasting [30,31,32,33]. Song et al. [34] empirically demonstrated that exposure of polyethylene and polypropylene pre-production pellets of mm dimensions to UV light and abrasive forces typical of a sandy temperate beach produced MP whose abundance increased with decreasing size. Given the dimensions of the majority of particles formed over an exposure period equivalent to several years in the environment (< 300 μm) and the depths to which UV oxidation can produce embrittlement of polymers (> 100 μm), significant weathering of fibrous and film-like MP is anticipated for equivalent timescales under much harsher desert conditions.

The surfaces of some MP examined by SEM, and in particular those from yardang hillsides, exhibited signs of intense photochemical and mechanical weathering, but surfaces of other MP appeared to be largely intact (Figure 3). This may partly reflect differences in resistance to particle abrasion among the different polymers, with polystyrene exhibiting a particularly low resistance in dry-sand abrasion tests [35] and revealing significant damage in desert soil (Figure 3d). More generally, however, these observations suggest that there may be two groups of MP in the desert environment. Firstly, MP that are subject to internal recycling (entrapment and redistribution) and pervasive weathering from more aggressive processes like sandblasting, impaction and burial. These MP may be relatively "old" and are likely to be associated with highly dynamic features and depositional zones such as moving sands and yardang hillsides[33]. Secondly, MP that are more transient and whose origins are more directly represented by recent back-trajectories. Here, more "juvenile" particles are carried through the desert relatively rapidly with the prevailing winds and may be intermittently entrained by temporary events or subject to less aggressive weathering processes like creep and saltation. Presumably, these different pathways and fates are determined

by the original properties of the plastics (e.g. size, shape, density) and regional variations in climate and geomorphology. However, further, longer-term studies would be required to verify this assertion and determine the precise drivers for differential particle behavior.

Photo-oxidation and mechanical weathering in the desert may also act to fractionate MP according to polymer strength, with less strong materials more readily fragmented into smaller particles (that are too small to be detected by our methodology). Thus, polymers having a relatively high tensile strength (PET = 55 MPa and Nylon = 70 MPa) were dominant amongst the desert MP characterized by μ-Raman spectroscopy while those of lower tensile strength (polypropylene and polystyrene, both 40 MPa) were present in only three cases. Significantly, polyethylene, the most widely produced thermoplastic but whose tensile strength is only 15 MPa, was entirely absent in the present study. By contrast, in remote soils impacted more by humidity and precipitation, polyethylene appears to make a much more important, and sometimes dominant contribution to the stock of detectable MP [9, 10].

In summary, the present study is the first to demonstrate the presence of MP in the subtropical desert environment. MP in soils from the Kavir and Lut deserts are dominated by fibres of various polymeric construction and are more concentrated on certain geomorphological features like the yardang hillsides. With little evidence of macro-plastics, it appears that MP are largely brought into the deserts from regional and more distant sources with the wind. Because some MP exhibit relatively little degradation yet others exhibit intense and heterogeneous weathering, it is proposed that there are two types of particle based on retention and fate. Thus, some MP are rather transient and are carried through the desert with relatively little interaction with surface features while others are internally recycled and are subject to significant photo-oxidation and mechanical weathering.

Supporting Information

UTM coordinates of the sampling locations and HYSPLIT model outputs for each month sampled in the Kavir desert are supplied as Supporting Information.

Acknowledgments

The authors would like to thank the Environmental Health Engineering Research Center, the Kerman University of Medical Sciences, for the financial support to carry out this project (No. 98000938).

References

(1) Zhou, Y., Liu, X., and Wang, J., 2018. Characterization of microplastics and the association of heavy metals with microplastics in suburban soil of central China. Science of the Total Environment 694, 133798.

(2) Choi, Y.R., Kim, Y.N., Yoon, J.H., Dickinson, N., Kim, K.H., 2020. Plastic contamination of forest, urban, and agricultural soils: A case study of Yeoju City in the Republic of Korea. Journal of Soils and Sediments DOI: 10.1007/s11368-020-02759-0

(3) Selonen, S., Dolar, A., Kokalj, A.J., Skalar, T., Dolcet, L.P., Hurley, R., van Gestel, C.A.M., 2020. Exploring the impacts of plastics in soil - The effects of polyester textile fibers on soil invertebrates. Science of the Total Environment 700, 134451.

(4) Ramos, L., Berenstein, G., Hughes, E. A., Zalts, A., and Montserrat, J. M., 2015. Polyethylene film incorporation into the horticultural soil of small periurban production units in Argentina, Science of the Total Environment 523, 74–81.

(5) Bläsing, M., Amelung, W., 2018. Plastics in soil: Analytical methods and possible sources, Science of the Total Environment 612, 422–435.

(6) Chen, Y., Leng, Y., Liu, X., Wang, J., 2019. Microplastic pollution in vegetable farmlands of suburb Wuhan, central China. Environmental Pollution 257, 113449.

(7) Büks, F., Kaupenjohann, M., 2020. Global concentrations of microplastics in soils – a review. SOIL 6, 649-662.

(8) Corradini, F., Casado, F., Leiva, V., Huerta-Lwanga, E., Geissen, V., 2021. Microplastics occurrence and frequency in soils under different land uses on a regional scale Science of the Total Environment 752, 141917.

(9) Feng, S.S., Lu, H.W. Tian, P.P., Xue, Y.X., Lu, J.Z., Tang, M., Feng, W., 2020. Analysis of microplastics in a remote region of the Tibetan Plateau: Implications for natural environmental response to human activities. Science of the Total Environment 739, 140087.

(10) Brahney, J., Hallerud, M., Heim, E., Hahnenberger, M., Sukumaran, S., 2020. Plastic rain in protected areas of the United States. Science 368, 1257-1260.

(11) Roblin, B., Ryan, M., Vreugdenhil, A., Aherne, J., 2020. Ambient atmospheric deposition of anthropogenic microfibers and microplastics on the western periphery of Europe (Ireland). Environmental Science and Technology 54, 11100-11108.

(12) Abbasi, S., Turner, A., submitted. Dry and wet deposition of microplastics in a semi-arid region (Shiraz, Iran). Submitted.

(13) Janhäll, S., 2015. Review on urban vegetation and particle air pollution – Deposition and dispersion. Atmospheric Environment 105, 130-137.

(14) Zylstra, E.R., 2015. Accumulation of wind-dispersed trash in desert environments. Journal of Arid Environments 89, 13-15.

(15) Mares, M.A., 1999 (editor). Encyclopedia of Deserts. University of Oklahoma Press, Norman, Oklahoma.

(16) UNESCO, 2016. Lut Desert. https://whc.unesco.org/en/list/1505 accessed 12/2020.

(17) Abbasi, H., 2019. Sand Dune Systems in Iran - Distribution and Activity. Wind Regimes, Spatial and Temporal Variations of the Aeolian Sediment Transport in Sistan Plain (East Iran). PhD Thesis, Fachbereich Geographie, Philipps-Universität Marburg.

(18) Abbasi, S., Keshavarzi, B., Moore, F., Turner, A., Kelly, F.J., Dominguez, A.O., Jaafarzadeh, N., 2019. Distribution and potential health impacts of microplastics and microrubbers in air and street dusts from Asaluyeh County, Iran. Environmental Pollution 244, 153–164.

(19) Zhang, D.D., Liu, X.D., Huang, W., Li, J.J., Wang, C.S., Zhang, D.S., Zhang, C.F., 2020. Microplastic pollution in deep-sea sediments and organisms of the Western Pacific Ocean. Environmental Pollution 259, 113948.

(20) Allen, S., Allen, D., Phoenix, V.R., Le Roux, G., Jimenez, P.D., Simonneau, A., Binet, S., Galop, D., 2019. Atmospheric transport and deposition of microplastics in a remote mountain catchment. Nature Geoscience 12, 339-344.

(21) Bergmann, M., Mützel, S., Primple, S., Tekman, M.B., Trachsel, J., Gerdts, G., 2019. White and wonderful? Microplastics prevail in snow from the Alps to the Arctic. Science Advances 5, eaax1157.

(22) Loppi, S., Roblin, B., Paoli, L., Aherne, J., 2021. Accumulation of airborne microplastics in lichens from a landfill dumping site (Italy). Scientific Reports 11, 4564.

(23) Pelletier, J. D., 2018. Controls on yardang development and morphology: 2. Numerical modeling. Journal of Geophysical Research: Earth Surface 123, 723–743.

(24) Dris, R., Gasperi, J., Mirande, C., Mandin, C., Guerrouache, M., Langlois, V., Tassin, B., 2017. A first overview of textile fibers, including microplastics, in indoor and outdoor environments. Environmental Pollution 221, 453-458.

(25) Bianco, A., Passananti, M., 2020. Atmospheric micro and nanoplastics: An enormous microscopic problem. Sustainability 12, 7327.

(26) Scheurer, M., Bigalke, M., 2018. Microplastics in Swiss floodplain soils. Environmental Science and Technology 52, 3591-3598.

(27) Evangeliou, N., Grythe, H., Klimont, Z., Heyes, C., Eckhardt, S., Lopez-Aparicio, S., and Stohl, A.: Atmospheric transport is a major pathway of microplastics to remote regions. Nature Communications 11, 1–11.

(28) Rezaei, M., Riksen, M.J.P.M., Sirjani, E., Sameni, A., Geissen, V., 2019. Wind erosion as a driver for transport of light density microplastics. Science of the Total Environment 669, 273-281.

(29) Corradini, F., Casado, F., Leiva, V., Huerta-Lwanga, E., Geissen, V., 2021. Microplastics occurrence and frequency in soils under different land uses on a regional scale Science of the Total Environment 752, 141917.

(30) Gomes, L., Bergametti, G., 1990. Submicron desert dusts: A sandblasting process. Journal of Geophysical Research 95, 13,927-13,935.

(31) Cordero, R.R., Damiani, A., Jorquera, J., Sepúlveda, E., Caballero, M., Fernandez, S., Feron, S., Llanillo, P.J., Carrasco, J., Laroze, D., Labbe, F., 2018. Ultraviolet radiation in the Atacama Desert. Antonie van Leeuwenhoek Journal of Microbiology 111, 1301-1313.

(32) Kheirabadi, H., Mahmoodabadi, M., Jalali, V. and Naghavi, H., 2018. Sediment flux, wind erosion and net erosion influenced by soil bed length, wind velocity and aggregate size distribution. Geoderma 323, 22-30.

(33) Ghodsi, M., 2017. Morphometric characteristics of Yardangs in the Lut Desert, Iran. Desert 22, 21-29.

(34) Song, Y.K., Hong, S.H., Jang, M., Han, G.M., Jung, S.W., Shim, W.J., 2017. Combined effects of UV exposure duration and mechanical abrasion on microplastic fragmentation by polymer type. Environmental Science and Technology 51, 4368-4376.

(35) Budinski, K.G., 1997. Resistance to particle Abrasion of selected plastics. Wear 203/204, 302-309.